

# Highly Sensitive Thermopile Sensors Using Nanostructured Si-Ge Thermoelectric Materials

Kyohei KAKUYAMA\*, Kotaro HIROSE, Masahiro ADACHI, Tsunehiro TAKEUCHI, and Masafumi KIMATA

This paper reports on the characteristics of a thermopile infrared sensor using nanostructured Si-Ge thermoelectric materials. While thermopile infrared sensors have the advantage of operating without power consumption, they have low sensitivity. To address this limitation, we have developed nanostructured Si-Ge thermoelectric materials that are expected to have a low thermal conductivity and a high Seebeck coefficient. With a thermal conductivity of 1/8 (0.8 W/(m·K)) and a Seebeck coefficient 2.8 times higher (330  $\mu\text{V/K}$ ) than that of conventional Si-Ge crystals, the nanostructured Si-Ge thermoelectric materials are expected to enhance the sensitivity of the thermopile infrared sensor. The thermopile infrared sensor using these materials achieved a sensitivity of 1,200 V/W at pressures below  $1 \times 10^{-1}$  Pa, demonstrating high sensitivity.

Keywords: thermopile infrared sensor, thermoelectric material, nanostructure, Si-Ge, high sensitivity

## 1. Introduction

Infrared sensors are used for various applications, including contactless body temperature measurement, which has attracted much public attention due to the COVID-19 pandemic, security in the industrial, consumer, and scientific fields, military operations, resource exploration, gas detection, diagnosis of architectural structures, vehicles, fire-fighting operations, and medical care. Infrared sensing technology has become increasingly important. Notably, the detection of medium- to long-wavelength infrared rays of 3 to 14  $\mu\text{m}$  makes it possible to detect human body temperature and harmful gases, including NOx. Accordingly, infrared sensing technology in this range is considered highly important.

Infrared sensors are classified into two major categories based on the detection method: quantum sensors and thermal sensors.<sup>(1)–(5)</sup> Quantum sensors are characterized by extremely high sensitivity. It should be noted, however, that they detect infrared rays by exciting electrons through infrared absorption of energy exceeding the band gap\*<sup>1</sup> of semiconductor materials. This means that the detectable infrared wavelengths are limited. In terms of the working principle, quantum sensors require a cooling mechanism, resulting in a large system and high cost. Regarding the detector materials, compound semiconductors, such as HgCdTe, are mainly used. Such materials pose problems because they are harmful and expensive.

There are four types of thermal sensors: thermopile<sup>(3),(6),(7)</sup>, bolometer<sup>(5)</sup>, diode<sup>(8)</sup> and pyroelectric<sup>(9)</sup> sensors. Unlike quantum sensors, none of these types of sensors require a cooling mechanism, making it possible to achieve low cost. However, thermal sensors have two main disadvantages: low response speed and sensitivity. We worked on the development of materials for a thermopile infrared sensor, a type of thermal infrared sensor that can be operated without power consumption, based on the belief that it would become possible to mount this type of sensor in mobile devices in the future if its sensitivity could be

improved. In this paper, we will explain our nanostructured Si-Ge thermoelectric materials<sup>(10),(11)</sup> and the characteristics of a thermopile infrared sensor developed by applying the materials.

## 2. Fabrication Process and Working Principle of Our Thermopile Infrared Sensor

Figure 1 shows the schematic diagram of our thermopile infrared sensor fabricated as a prototype. After forming a supporting film, which was made from SiN or SiO<sub>2</sub>, on a Si substrate, n-type and p-type thermoelectric materials were arranged in a  $\pi$  shape. An infrared absorption film capable of absorbing infrared rays and converting them into heat was then formed on the thermoelectric materials. Subsequently, the thickness of the substrate was reduced by dry etching from the reverse side to suppress the outflow of heat to the substrate.

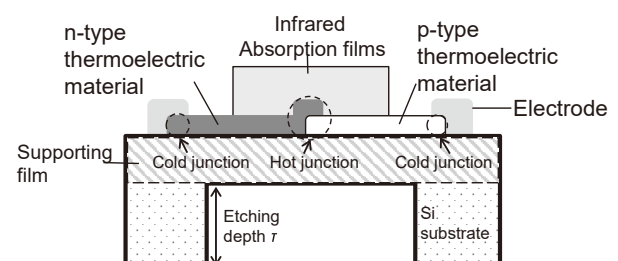


Fig. 1. Cross section of the thermopile sensor

When the infrared absorption film absorbs infrared rays, the temperature at the center of the sensor, where the hot junction is located, increases. On the other hand, the

temperature of the cold junctions, which are formed on the substrate side, remains almost unchanged. This leads to a temperature difference between the junctions, generating voltage at both ends of the thermocouple. Pairs of n-type and p-type thermoelectric materials are connected in series to obtain the sum of the thermo electromotive force generated by each pair. The sensitivity of the thermopile infrared sensor  $S_V$  can be expressed by the Eq. (1). (As discussed below, for simplification, the equation is based on the assumption that there is no influence of heat transfer by radiation.)

$$S_V \approx N (\alpha_p - \alpha_n) R_{th} \propto (\alpha_p - \alpha_n) / \kappa_{th} \dots\dots\dots (1)$$

Here,  $N$  is the number of thermoelectric material pairs,  $\alpha_p$  and  $\alpha_n$  are Seebeck coefficients\*2 of the p-type and n-type thermoelectric materials,  $R_{th}$  is the thermal resistance of the thermopile infrared sensor, and  $\kappa_{th}$  is the thermal conductivity of the thermoelectric materials.  $R_{th}$  is determined by the thermal conductivity of the supporting film, which is made from  $\text{SiO}_2$  or  $\text{SiN}$ , and the thermoelectric materials.  $R_{th}$  is roughly in inverse proportion to the thermal conductivity  $\kappa_{th}$  of the thermoelectric materials. Thus, to realize a high-sensitivity thermopile infrared sensor, it is required to achieve both low thermal conductivity and a high Seebeck coefficient for thermoelectric materials.

### 3. Nanostructured Si-Ge Thermoelectric Materials

#### 3-1 Reduction in thermal conductivity by using nanostructures

We developed nanostructured Si-Ge thermoelectric materials that ensure both low thermal conductivity and a high Seebeck coefficient. First, the method of reducing the thermal conductivity is explained.

The thermal conductivity  $\kappa_{th}$  of the thermoelectric materials is expressed by the Eq. (2) using the thermal conductivity by electrons  $\kappa_{ele}$  and the thermal conductivity by phonons  $\kappa_{lat}$ <sup>(12)</sup>.

$$\kappa_{th} = \kappa_{ele} + \kappa_{lat} \dots\dots\dots (2)$$

$\kappa_{ele}$  is reducible by reducing the transport of electrons in materials. However, this measure increases the electrical resistance of a thermopile infrared sensor. Thus, we focused on reducing  $\kappa_{lat}$  instead of  $\kappa_{ele}$ . In general, to reduce  $\kappa_{lat}$ , there is a technique to scatter phonons, which transport heat, by nanostructures formed in materials.<sup>(10)-(15)</sup> Previous research used structures, including superlattices,<sup>(13)</sup> nanowires,<sup>(14)</sup> and quantum dots.<sup>(15)</sup> We deposited nanocrystals in the mother phase with amorphous structures by using a technique to perform heat treatment of thermoelectric materials with amorphous structures. The nanostructures increased the scattering of phonons, leading to a significant reduction in the lattice thermal conductivity.<sup>(16)</sup> Compared to other techniques, this technique can increase the volume of nanostructures only by simple heat treatment and therefore excels in productivity.<sup>(17)</sup> A cross-sectional TEM image of the nanostructured Si-Ge that we fabricated is shown in

Fig. 2. Regions encircled by white dashed lines, where regular atomic arrays are observed, represent nanocrystals. Regions outside the circles are the mother phase of the amorphous structure.

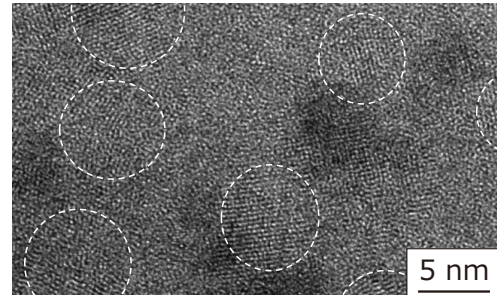


Fig. 2. Cross-sectional TEM image of the nanostructured Si-Ge thermoelectric material

Figure 3 shows thermal conductivity's dependence on the nanocrystal grain size of the nanostructured Si-Ge thermoelectric materials. For nanostructured Si-Ge, a low thermal conductivity of 1 W/(m·K) or less can be attained by reducing the mean grain size to 5 nm or less. The thermal conductivity is one-eighth that of conventional monocrystalline Si-Ge.<sup>(10)-(12)</sup>

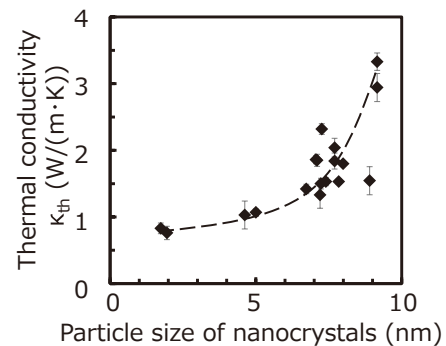


Fig. 3. Thermal conductivity's dependence on the nanocrystal grain size of nanostructured Si-Ge thermoelectric materials

#### 3-2 Improvement of the Seebeck coefficient by co-doping

Next, we explain the method of improving the Seebeck coefficient of nanostructured Si-Ge thermoelectric materials. The Seebeck coefficient is known to be dependent on the energy of electrons in materials. It is particularly important to control electrons that have energy near the Fermi level  $E_F$  (within  $\pm 5 k_B T$ ).<sup>(18),(19)</sup> Here,  $k_B$  is the Boltzmann constant, and  $T$  is the temperature. To control the electronic structure, we used co-doping technology, in which two elements are added to materials.<sup>(18),(19)</sup> Co-doping plays two roles. One is to form an impurity level, whose energy width is narrow, near the band edge, and the other is to adjust the Fermi level near the new level. First, we performed the first-principles calculation to determine an

element that would form the desired new level. As a result, it was found effective to add several at.% of Au.<sup>(18)</sup> For adjustment of the Fermi level, we used B, which can be replaced by Si and Ge. We fabricated a specimen by co-doping Au and B and conducted an evaluation. We confirmed that the Seebeck coefficient improved to 330  $\mu\text{V/K}$ , which was 2.8 times that of monocrystalline Si-Ge, while maintaining low thermal conductivity.<sup>(20)</sup>

#### 4. Comparison with Other Materials

Figure 4 shows the results of comparison of room temperature characteristics between conventional thermoelectric materials (Al, poly-Si, Bi, Sb, and Si-Ge), which are used for thermopile infrared sensors, and nanostructured Si-Ge thermoelectric materials.<sup>(21)–(24)</sup> The dashed lines in the figure show expected sensitivity values that are calculated based on the assumption that thermopile infrared sensors are of the same relatively simple structure. The figure shows that the thermal resistivity and Seebeck coefficient of the nanostructured Si-Ge thermoelectric materials have dramatically improved compared to those of the conventional materials. Application of the new materials is expected to achieve a sensitivity of 1,000 V/W or more, which is 10 times or more than that of the conventional materials, for thermopile infrared sensors.

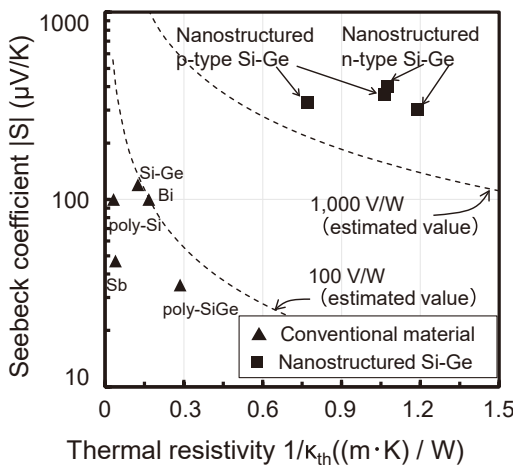


Fig. 4. Comparison of the room temperature characteristics of thermoelectric materials used for thermopile infrared sensors (The dashed line shows the estimated value of sensor sensitivity for the same structure.)

#### 5. Influence on Sensitivity Due to Heat Radiation to the Gaseous Body

##### 5-1 Analysis of heat transfer paths

When using a thermoelectric material whose thermal conductivity is lower than that of conventional thermoelectric materials, the decrease in sensor sensitivity due to heat radiation to the surroundings from the infrared absorption film, which absorbs infrared rays and generates heat, cannot be ignored. Thus, to realize a high-sensitivity thermopile infrared sensor that unleashes the high potential of

nanostructured Si-Ge thermoelectric materials, it is necessary to ensure control to prevent radiation of heat generated by infrared absorption.<sup>(25)</sup> Here, we introduce a physical model that takes into account the heat transfer paths of a thermopile infrared sensor.

As shown in Fig. 1, heat absorbed by the infrared absorption film flows in three paths: (i) thermoelectric materials and supporting film, (ii) radiation to the surroundings, and (iii) gaseous body present around the sensor. The thermal conductance\*<sup>3</sup> of each path ( $G_{sup}$ ,  $G_{rad}$ , and  $G_{gas}$ ) can be expressed as Eqs. (3)–(6).<sup>(25),(26)</sup>

$$G_{gas} = \frac{\kappa_{gas}(p) \times A_d}{\tau} \dots\dots\dots (3)$$

$$G_{rad} = 4 \times \sigma_{sb} \times A_d \times T_d^3 \dots\dots\dots (4)$$

$$G_{all} = G_{sup} + G_{gas} + G_{rad} = \frac{1}{R_{th}} \dots\dots\dots (5)$$

$$\kappa_{gas} = \frac{\kappa_0 + \kappa_{flow}}{1 + \frac{7.6 \times 10^{-5}}{p \times \frac{\tau}{T_d}}} \dots\dots\dots (6)$$

Here,  $\kappa_{gas}$  is the effective thermal conductivity of the gaseous body with convection taken into account,  $p$  is the pressure,  $\tau$  is the etching depth,  $A_d$  is the detector area,  $\sigma_{sb}$  is the Stefan-Boltzmann constant,  $T_d$  is the temperature of the light receiving unit,  $\kappa_0$  is the effective thermal conductivity of the atmosphere, and  $\kappa_{flow}$  is the effective thermal conductivity by convection.  $G_{all}$  is the total thermal conductance of a thermopile infrared sensor. The sensitivity of a thermopile infrared sensor is in inverse proportion to  $G_{all}$ . Most components of  $G_{all}$  are attributed to the sensor structure. To improve sensitivity for the same structure, it is necessary to reduce  $G_{gas}$ . To this end, the pressure of the gaseous body surrounding a sensor must be reduced close to the vacuum.

##### 5-2 Demonstration of high sensitivity by a high degree of vacuum

To verify the physical model in the previous section, we placed a thermopile infrared sensor in the vacuum equipment and measured the output voltage of the sensor while changing the pressure in the equipment with the sensor being irradiated with infrared rays. The results of the comparison between the experiment values and the calculation values obtained by Eqs. (3)–(6) are shown in

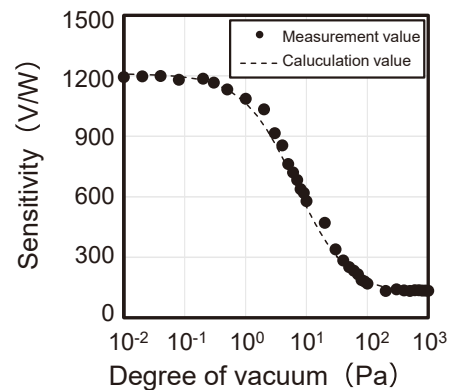


Fig. 5. Sensitivity's dependence on the degree of vacuum for thermopile infrared sensors

Fig. 5. The actual measurement values matched well with the calculation values. With the pressure below  $1 \times 10^2$  Pa, the sensor sensitivity started to increase and reached 1,200 V/W at  $1 \times 10^{-1}$  Pa or less. We demonstrated that a high-sensitivity thermopile infrared sensor can be realized by using nanostructured Si-Ge thermoelectric materials whose physical properties are reformed to conform to the requirements of thermopile infrared sensors.

## 6. Conclusion

In this paper, we fabricated a thermopile infrared sensor that is expected to achieve high sensitivity by using nanostructured Si-Ge thermoelectric materials whose thermal conductivity is one-eighth that of conventional Si-Ge crystals ( $0.8 \text{ W}/(\text{m}\cdot\text{K})$ ) and whose Seebeck coefficient is 2.8 times that of conventional Si-Ge crystals ( $330 \mu\text{V}/\text{W}$ ). The sensitivity of this sensor reached up to 1,200 V/W at the ambient pressure of  $1 \times 10^{-1}$  Pa or less. To verify the physical properties of the materials, we developed a thermopile infrared sensor with a simple structure. To develop sensors of higher performance, it is necessary to improve both the materials and the sensor structure. Candidate solutions include the application of a supporting structure, which is used for array sensors, and an umbrella structure, which can increase the area of the infrared absorption film,<sup>(27)</sup> reduction in thickness of the supporting film, and introduction of phononic crystals to the supporting film and thermoelectric materials.<sup>(28),(29)</sup> Further study on such development is underway.

## 7. Acknowledgments

In the research and development, we received valuable advice from Professor Okamoto of the National Defense Academy of Japan. We express our deepest appreciation.

### Technical Terms

- \*1 Band gap: A difference in energy between the conduction band and the valence band in a crystal. The band gap is specific to respective materials. The magnitude of the band gap is used in optical devices that emit or absorb light at specific wavelengths.
- \*2 Seebeck coefficient: An index that indicates the magnitude of voltage generated depending on the temperature difference of an overall material. A high value is expected to realize a highly sensitive thermopile sensor.
- \*3 Thermal conductance: A reciprocal of thermal resistance. It indicates the ease of heat flow.

### References

- (1) A. Rogalski, and K. Chrzanowski, in *Infrared Devices and Techniques*, 2nd ed. (Optoelectronics Review, 2002), pp. 111–136
- (2) A.W. Van Herwaarden, and P.M. Sarro, in *Thermal Sensors Based on the Seebeck Effect* (Sens. Actuators, 1986), pp. 321–346
- (3) A. Graf, M. Arndt, M. Sauer, and G. Gerlach, “Review of micromachined thermopiles for infrared detection,” *Meas. Sci. Technol.* 18(7), R59–R75 (2007)
- (4) A. Rogalski, “Quantum well photoconductors in infrared detector technology,” *Journal of Applied Physics* 93(8), 4355–4391 (2003)
- (5) P.L. Richards, “Bolometers for infrared and millimeter waves,” *Journal of Applied Physics* 76(1), 1–24 (1994)
- (6) E.M. Barrentine, A.D. Brown, C.A. Kotecki, V. Mikula, R.A. Reid, S.H. Yoon, and A.T. Joseph, in *Image Sensing Technologies: Materials, Devices, Systems, and Applications VI*, edited by N.K. Dhar, A.K. Dutta, and S.R. Babu (SPIE, Baltimore, United States, 2019), p. 13
- (7) S.B. Mbarek, N. Alcheikh, and M.I. Younis, “Recent advances on MEMS based Infrared Thermopile detectors,” *Microsyst Technol* 28, 1751–1764 (2022)
- (8) M. Mansoor, I. Haneef, S. Akhtar, A. De Luca, and F. Udrea, “Silicon diode temperature sensors—A review of applications,” *Sensors and Actuators A: Physical* 232, 63–74 (2015)
- (9) A. Sixsmith, N. Johnson, and R. Whatmore, “Pyroelectric IR sensor arrays for fall detection in the older population,” *J. Phys. IV France* 128, 153–160 (2005)
- (10) M. Adachi, et al., “Control of Nano Structure by Multi Films for Nano-structured Thermoelectric Materials,” *SEI TECHNICAL REVIEW*, No.84 (April 2017)
- (11) S. Nishino, S. Ekino, M. Inukai, M. Omprakash, M. Adachi, M. Kiyama, Y. Yamamoto, and T. Takeuchi, “Thermoelectric Properties of Nanograined Si-Ge-Au Thin Films Grown by Molecular Beam Deposition,” *Journal of Elec Materials* 47(6), 3267–3272 (2018)
- (12) K. Hirose, M. Adachi, M. Murata, Y. Yamamoto, and T. Takeuchi, in *Quantum Sensing and Nano Electronics and Photonics XVII*, edited by M. Razeghi, J.S. Lewis, G.A. Khodaparast, and P. Khalili (SPIE, San Francisco, United States, 2020), p. 19
- (13) H. Böttner, G. Chen, and R. Venkatasubramanian, “Aspects of Thin-Film Superlattice Thermoelectric Materials, Devices, and Applications,” *MRS Bull.* 31(3), 211–217 (2006)
- (14) N. Samaraweera, J.M. Larkin, K.L. Chan, and K. Mithraratne, “Reduced thermal conductivity of Si/Ge random layer nanowires: A comparative study against superlattice counterparts,” *Journal of Applied Physics* 123(24), 244303 (2018)
- (15) D. Yang, C. Lu, H. Yin, and I.P. Herman, “Thermoelectric performance of PbSe quantum dot films,” *Nanoscale* 5(16), 7290 (2013)
- (16) H. Takiguchi, M. Aono, and Y. Okamoto, “Nano Structural and Thermoelectric Properties of SiGeAu Thin Films,” *Jpn. J. Appl. Phys.* 50(4), 041301 (2011)
- (17) P. Jood, M. Ohta, A. Yamamoto, and M.G. Kanatzidis, “Excessively Doped PbTe with Ge-Induced Nanostructures Enables High-Efficiency Thermoelectric Modules,” *Joule* 2(7), 1339–1355 (2018)
- (18) M. Adachi, S. Nishino, K. Hirose, M. Kiyama, Y. Yamamoto, and T. Takeuchi, “High Dimensionless Figure of Merit  $ZT = 1.38$  Achieved in p-Type Si-Ge-Au-B Thin Film,” *Mater. Trans.* 61(5), 1014–1019 (2020)
- (19) T. Takeuchi, “Conditions of Electronic Structure to Obtain Large Dimensionless Figure of Merit for Developing Practical Thermoelectric Materials,” *Mater. Trans.* 50(10), 2359–2365 (2009)
- (20) H. Lai, Y. Peng, J. Gao, H. Song, M. Kurosawa, O. Nakatsuka, T. Takeuchi, and L. Miao, “Reinforcement of power factor in N-type multiphase thin film of Si  $1-x-y$  Ge  $x$  Sn  $y$  by mitigating the opposing behavior of Seebeck coefficient and electrical conductivity,” *Appl. Phys. Lett.* 119(11), 113903 (2021)
- (21) P.G. Klemens, and T.K. Chu, *Thermal Conductivity* 14 (Springer, Boston, 2013)
- (22) B. Abeles, and R.W. Cohen, “Ge-Si Thermoelectric Power Generator,” *Journal of Applied Physics* 35(1), 247–248 (1964)
- (23) M. Strasser, R. Aigner, C. Lauterbach, T.F. Sturm, M. Franosch, and G. Wachutka, “Micromachined CMOS thermoelectric generators as on-chip power supply,” *Sensors and Actuators A: Physical* 114(2–3), 362–370 (2004)
- (24) C.F. Gallo, B.S. Chandrasekhar, and P.H. Sutter, “Transport Properties of Bismuth Single Crystals,” *Journal of Applied Physics* 34(1), 144–152 (1963)

- (25) H. Wu, S. Grabarnik, A. Emadi, G. de Graaf, and R.F. Wolffenbuttel, "Characterization of thermal cross-talk in a MEMS-based thermopile detector array," *J. Micromech. Microeng.* 19(7), 074022 (2009)
- (26) M. Kimata, "Infrared sensors Principle and technology", Kagakujiyoho shuppan Co., Ltd., Tsukuba (2018), pp. 34-36
- (27) M. Kimata, "Uncooled infrared focal plane arrays: UNCOOLED INFRARED FOCAL PLANE ARRAYS," *IEEJ Trans Elec Electron Eng* 13(1), 4-12 (2018)
- (28) N. Tambo, K. Takahashi, K. Nakamura, Y. Naito, E.M. Ashley, P.J. Duda, P.F. Nealey, and M. Fujikane, in *Image Sensing Technologies: Materials, Devices, Systems, and Applications VIII*, edited by N.K. Dhar, A.K. Dutta, and S.R. Babu (SPIE, Online Only, United States, 2021), p. 3
- (29) K.F. Gray, J.F. Muth, and W. Carr, in *2016 IEEE SENSORS (IEEE, Orlando, FL, USA, 2016)*, pp. 1-3

**Contributors** The lead author is indicated by an asterisk (\*).

**K. KAKUYAMA\***

• Transmission Devices Laboratory



**K. HIROSE**

• Transmission Devices Laboratory



**M. ADACHI**

• Doctor of Engineering  
Senior Assistant Manager, Transmission Devices  
Laboratory



**T. TAKEUCHI**

• Doctor of Engineering  
Professor, Toyota Technological Institute



**M. KIMATA**

• Doctor of Engineering  
Technical consultant,

